

Variational Wasserstein Clustering

Liang Mi¹, Wen Zhang¹, Xianfeng Gu², Yalin Wang¹

¹ Arizona State University, ² Stony Brook University

Abstract. We propose a new clustering method based on optimal transportation. We solve optimal transportation with variational principles, and investigate the use of power diagrams as transportation plans for aggregating arbitrary domains into a fixed number of clusters. We iteratively drive centroids through target domains while maintaining the minimum clustering energy by adjusting the power diagrams. Thus, we simultaneously pursue clustering and the Wasserstein distances between centroids and target domains, resulting in a robust measure-preserving mapping. In general, there are two approaches for solving optimal transportation problem – Kantorovich’s v.s. Brenier’s. While most researchers focus on Kantorovich’s approach, we propose a solution to clustering problem following Brenier’s approach and achieve a competitive result with the state-of-the-art method. We demonstrate our applications to different areas such as domain adaptation, remeshing, and representation learning on synthetic and real data.

Keywords: Optimal transportation, Wasserstein distance, measure preserving, clustering, discrete distribution, k-means

1 Introduction

Aggregating distributional data into clusters has ubiquitous applications in computer vision and machine learning. A continuous example is unsupervised image categorization and retrieval where similar images reside close to each other in the image space or the descriptor space and they are clustered together and form a specific category. A discrete example is document or speech analysis where words and sentences that have similar meanings are often grouped together. k-means [1,2] is one of the most famous clustering algorithms which aims to partition empirical observations into k clusters in which each observation has the closest distance to the *mean* of its own cluster. It was originally developed for solving quantization problems in signal processing and in early 2000s researchers have discovered its connection to another classic algorithm optimal transportation which seeks an optimal transportation plan that minimizes the transportation cost between probability measures [3].

The optimal transportation (OT) problem has received great attention since its very birth. Numerous applications such as color transfer and shape retrieval have benefited from solving OT between probability distributions. Furthermore, by regarding the minimum transportation cost – *the Wasserstein distance* – as

a metric, researchers have been able to compute the barycenter [4] of multiple distributions, e.g. [5,6]. Most researchers regard OT as finding the optimal coupling of the two probabilities and thus each sample can be mapped to multiple places. It is often called Kantorovich OT. Along this direction, several works have shown their high performance in clustering distributional data via optimal transportation, e.g. [7,6,8]. On the other hand, some researchers regard OT as a measure-preserving mapping between distributions and thus the mass cannot be split. It is called Monge-Brenier OT.

In this paper, we propose a clustering method from Monge-Brenier’s approach. Our method is based on Gu *et al.* [9] which provides a variational solution to Monge-Brenier OT problem. We call it *variational optimal transportation* and name our method *variational Wasserstein clustering*. We leverage the connection between *the second-order Wasserstein distance* and the clustering error function, and simultaneously pursue the Wasserstein distance and the k-means clustering by using a power Voronoi diagram. Given the empirical measure of a target probability distribution, we start from a sparse discrete measure as the initial guess of the centroids and iteratively update the centroids while maintaining an optimal transportation plan. From a computational point of view, our method is solving a special case of the *Wasserstein barycenter* problem [4,5] when the target is a univariate measure. We demonstrate the applications of our method to three different tasks – domain adaptation, remeshing, and representation learning. In domain adaptation on synthetic data, we achieve the competitive results with JDOT [10], an method from Kantorovich’s approach. To the best of our knowledge, this is the first attempt of solving clustering problems from the perspective of Monge-Brenier optimal transportation. The advantages of our approach over those based on Kantorovich’s formulation are that (1) it is a local diffeomorphism; (2) it does not require pre-calculated pairwise distances; and (3) it avoids searching in the product space and thus dramatically reduces the number of parameters.

The rest of the paper is organized as follows. In Section 2 and 3, we provide the related work and preliminaries on optimal transportation and k-means clustering. In Section 4, we present the variational principles for solving optimal transportation. In Section 5, we introduce our formulation of the k-means clustering problem under variational Wasserstein distances. In Section 6, we show the experiments and results from our method on different tasks. Finally, we conclude our work in Section 7 with future directions.

2 Related Work

2.1 Optimal Transportation

The optimal transportation (OT) problem was originally raised by Monge [11] in 18th century, which sought a transportation plan for matching distributional data with the minimum cost. In 1941, Kantorovich [12] introduced a relaxed version and proved its existence and uniqueness. Kantorovich also provided an

optimization approach based on linear programming, which has become the dominant direction. Traditional ways of solving the Kantorovich’s OT problem rely on pre-defined pairwise transportation costs between measure points, e.g. [13], while recently researchers have developed fast approximations that incorporate computing the costs within their frameworks, e.g. [6]. Meanwhile, another line of research followed Monge’s OT problem and had a breakthrough in 1987 when Brenier [14] discovered the intrinsic connection between optimal transportation and convex geometry. Following Brenier’s theory, Gu *et al.* [9] introduced a variational solution to Monge’s OT problem by leveraging power Voronoi diagrams and Su *et al.* [15] provided computational algorithms to solve Monge’s OT problem on surfaces.

2.2 Wasserstein Metrics

The Wasserstein distance is the minimum cost induced by the optimal transportation plan. It satisfies all metric axioms and thus is often borrowed for measuring the similarity between probability distributions. The transportation cost generally comes from the product of the geodesic distance between two sample points and their measures. We refer to p -Wasserstein distances to specify the exponent p when calculating the geodesic [16]. The 1-Wasserstein distance or earth mover’s distance (EMD) has received great attention in image and shape comparison [17,18]. Along with the rising of deep learning in numerous areas, 1 -Wasserstein distances have been adopted in many ways for designing loss functions for its robustness over other measures [19,20,21]. The 2-Wasserstein distance, although requiring more computation, are also popular in image and geometry processing thanks to its geometric properties such as barycenters [4,6]. In this paper, we focus on 2-Wasserstein distances.

2.3 K-means Clustering

The K-means clustering method goes back to Lloyd [1] and Forgy [2]. Its connections to the 1, 2-Wasserstein metrics was leveraged in [8] and [22], respectively. The essential idea is to use a sparse discrete point set to cluster denser or continuous distributional data with respect to the Wasserstein distance between the original data and the sparse representation, which is equivalent to finding a Wasserstein barycenter when $N = 1$ [5]. A few other works have also contributed to this problem by proposing fast optimization methods, e.g. [7].

In this paper, we approach the k-means problem from the perspective the optimal transportation in variational principles. Since we leverage power diagrams to compute optimal transportation, we simultaneously pursue the Wasserstein distance and k-means clustering. We compare our method with other ones from a conceptual point of view and through empirical experiments and demonstrate its effectiveness in computer vision and machine learning research.

3 Preliminaries

We first introduce the optimal transportation (OT) problem and then show its connection to k-means clustering. We use $X(x, \mu)$ to represent a metric space $X(x)$ with measure $\mu(x)$, and $X(\mathbf{x}, \boldsymbol{\mu})$ to indicate that the $\boldsymbol{\mu}$ is discretely supported at \mathbf{x} .

3.1 Optimal Transportation

Suppose $X(x, \mu)$ and $Y(y, \nu)$ are two metric spaces with *Borel* probability measures that satisfy $\int_X \mu(x) dx = \int_Y \nu(y) dy$, $\mu(x), \nu(y) > 0$. We say a mapping $T : X(x, \mu) \rightarrow Y(y, \nu)$ is measure preserving if the measure of any subset B of Y is equal to the measure of the origin of B in X , which means $\mu(T^{-1}(B)) = \nu(B)$, $\forall B \subset Y$. We can regard T as the *coupling* $\pi(x, y)$ of the two measures, each being a corresponding *marginal* $\mu = \pi(\cdot, y)$, $\nu = \pi(x, \cdot)$. Then, all the couplings are the probability measure in the product space, $\pi \in \prod(X \times Y)$. Given a transportation cost $c : X \times Y \rightarrow \mathbb{R}^+$ — usually the geodesic distance to the moment of p , $c(x, y) = d^p(x, y)$ — the problem of optimal transportation (OT) is to find the measure-preserving mapping $\pi_{opt} : X \rightarrow Y$ that minimizes the total cost,

$$W_p(\mu, \nu) \stackrel{\text{def}}{=} \left(\inf_{\pi \in \prod(\mu, \nu)} \int_{X \times Y} c(x, y) d\pi(x, y) \right)^{1/p}. \quad (1)$$

where p indicates the moment. We call the minimum total cost the p – *Wasserstein distance*. Since we address the original Monge’s OT problem in which the mass cannot be split, we thus have the restriction that $d\pi(x, y) = d\pi_T(x, y) \equiv d\mu(x)\delta[y = T(x)]$, inferring that

$$\pi_{T_{opt}} = T_{opt} = \arg \min_T \int_X c(x, T(x)) d\mu(x). \quad (2)$$

In this paper, we follow Eq. (2). The details of the optimal transportation problem and the properties of the Wasserstein distance can be found in [23,21]. For simplicity, T_{opt} is replaced by T .

3.2 K-means Clustering

Given the empirical measures $\{(x_i, \mu_i)\}$ of a probability distribution X , the k-means clustering problem seeks to assign a cluster centroid (or prototype) $y_j = y(x_i)$ with label $j = 1, \dots, k$ to each empirical sample x_i in such a way that the error function (3) reaches its minimum and meanwhile $\nu_j = \sum_{y_j = y(x_i)} \mu_i$. It is equivalent to finding a partition $V = \{(V_j, y_j)\}$ of the embedding space M . If M is convex, then so is V_j .

$$\arg \min_y \sum_{x_i} \mu_i \|x_i - y(x_i)\|^2 \equiv \arg \min_V \sum_{j=1}^K \sum_{x_i \in V_j} \mu_i \|x_i - y(V_j)\|^2. \quad (3)$$

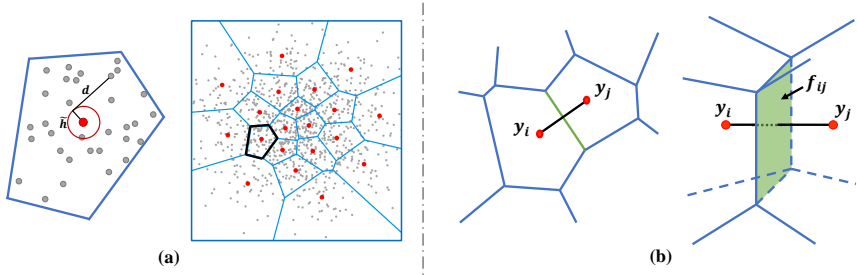


Fig. 1. (a) Power Voronoi diagram. Red dots are centroids of the Voronoi cells, or clusters. The transportation cost is the product of the the measure of a sample and its power distance to its own centroid. (b) shows the intersection between adjacent cells in 2D and 3D. Hessian is calculated according to the geometric relation near intersections.

Such a clustering problem (3), when ν is fixed, is equivalent to Monge’s OT problem (2) when the support of \mathbf{y} is sparse and not fixed. Therefore, the solution to Eq. (3) comes from the optimization in the search space $P(\mathbf{y}, V)$. Note that when ν is not fixed such a problem becomes a Wasserstein barycenter problem as finding a solution in $P(\mathbf{y}, \nu, V)$, studied in [4,5,7].

4 Variational Optimal Transportation

We present the variational principles for solving the discrete optimal transportation problem. Given a metric space $X(x)$, a Borel probability measure $\mu(x)$, and its compact support $\Omega = \text{supp } \mu = \{x \in X \mid \mu(x) > 0\}$, we consider a sparsely supported point set with Dirac measure $Y(\mathbf{y}, \nu) = \{(y_j, \nu_j > 0)\} \subset X(x, \mu)$, $j = 1, \dots, K$. Our goal is to find an optimal transportation plan or map (OT-map), $\pi : x \rightarrow \mathbf{y}$, with the *push-forward* $\pi_{\#}\mu = \nu$. This is *semi-discrete OT*. We introduce a height vector $\mathbf{h} = (h_1, \dots, h_k)^T$, and a hyperplane on X , $\gamma_j(\mathbf{h}) : \langle x, y_j \rangle + h_j = 0$. Then, the following function is convex.

$$\theta_{\mathbf{h}}(x) = \max\{\langle x, y_j \rangle + h_j\}, \quad j = 1, \dots, K.$$

From Aurenhammer [24], we know that a convex subdivision associated to a piece-wise linear convex function $u_{\mathbf{h}}(x)$ on \mathbb{R}^n equals a *power Voronoi diagram*, Ω :

$$\Omega = \bigcup V_i(\mathbf{h}), \quad j = 1, \dots, K,$$

where each cell, $V_j(\mathbf{h}) = \{x \in X \mid \theta_{\mathbf{h}}(x) = \langle x, y_j \rangle + h_j\}$, is the projection of a facet of $G(\mathbf{h})$. The following theorem plays the fundamental role in our formulation.

Theorem 1. (Alexandrove [25]) *Suppose Ω is a compact convex polytope with non-empty interior in \mathbb{R}^n and $y_1, \dots, y_k \subset \mathbb{R}^n$ are distinct k points and $\nu_1, \dots, \nu_k > 0$ so that $\sum_{i=1}^k \nu_i = \text{vol}(\Omega)$. There exists a unique vector $\mathbf{h} = (h_1, \dots, h_k)^T \in \mathbb{R}^k$*

Algorithm 1: Variational optimal transportation

Function Variational-OT($X(\mathbf{x}, \boldsymbol{\mu}), Y(\mathbf{y}, \mathbf{v}), \epsilon, \sigma$)

 $\mathbf{h} \leftarrow \mathbf{0}$.

repeat

 Update power diagram \mathbf{V} with (\mathbf{y}, \mathbf{h}) .

 Compute cell weight $w(\mathbf{h}) = \{\sum_{m \in V_i} \mu(m)\}$.

 Compute $\nabla E(\mathbf{h})$ and H using Equation (5) and (6).

 $\mathbf{h} \leftarrow \mathbf{h} - \lambda H^{-1} \nabla E(\mathbf{h})$. // Update the minimizer \mathbf{h}
until $|\nabla E(\mathbf{h})| < \epsilon$.

return \mathbf{V}, \mathbf{h} .

end

up to a translation factor $(c, \dots, c)^T$ such that the piecewise linear convex function $\theta_{\mathbf{h}}(x) = \max_{x \in \Omega} \{ \langle x, y_j \rangle + h_j \}$ satisfies $\text{vol}(x \in \Omega \mid \nabla \theta_{\mathbf{h}}(x) = y_j) = \nu_j$.

Furthermore, Brenier [14] proved that the gradient map $\nabla \theta$ provides the solution to Monge's OT problem that is $\nabla \theta_{\mathbf{h}}$ minimizes the transportation cost $\int_{\Omega} \|x - \theta_{\mathbf{h}}(x)\|^2$. Therefore, \mathbf{h} , and \mathbf{h} alone, induces the OT-Map.

We can determine $V_j(h)$ by the *power distance* $\|x_i - y_j\|^2 + \tilde{h}_j$ where $\tilde{h}_j = 2h_j + \|y_j\|^2$. Now, we introduce an energy function

$$\begin{aligned} E(\mathbf{h}) &\stackrel{\text{def}}{=} \int_{\Omega} \theta_{\mathbf{h}}(x) \mu(x) dx - \sum_{j=1}^K \nu_j h_j \\ &\equiv \int_{\mathbf{h}} \sum_{j=1}^K w_j(\xi) d\xi - \sum_{j=1}^K \nu_j h_j. \end{aligned} \quad (4)$$

E is differentiable w.r.t. \mathbf{h} [9]. Its gradient and Hessian are then given by

$$\nabla E(\mathbf{h}) = (w_1(\mathbf{h}) - \nu_1, \dots, w_l(\mathbf{h}) - \nu_K)^T, \quad (5)$$

$$H = \frac{\partial^2 E(\mathbf{h})}{\partial h_i \partial h_j} = \begin{cases} \sum_k \frac{\int_{f_{ik}} \mu(x) dx}{\|y_k - y_i\|}, & i = j, \forall k, \text{ s.t. } f_{ik} \neq \emptyset, \\ -\frac{\int_{f_{ij}} \mu(x) dx}{\|y_j - y_i\|}, & i \neq j, f_{ij} \neq \emptyset, \\ 0, & i \neq j, f_{ij} = \emptyset, \end{cases} \quad (6)$$

where $\|\cdot\|$ is the $L1$ norm and $\int_{f_{ij}} \mu(x) dx = \text{vol}(f_{ij})$ is the volume of the intersection. Fig. 1 (b) illustrates the geometric relation. The Hessian H is positive semi-definite with only constant functions spanned by a vector $(1, \dots, 1)^T$ in its null space. Thus E is convex in \mathbf{h} . By Newton's method, we solve a linear system,

Algorithm 2: Iterative measure-preserving mapping (IMPM)

```

Function Iterative-Measure-Preserving-Mapping( $X(\mathbf{x}, \boldsymbol{\mu}), Y(\mathbf{y}, \boldsymbol{\nu})$ )
  repeat
    |  $\mathbf{V}(\mathbf{h}) \leftarrow$  Variational-OT( $\mathbf{x}, \boldsymbol{\mu}, \mathbf{y}, \boldsymbol{\nu}$ ). // 1. Update Voronoi partition
    |  $\mathbf{y}_j \leftarrow \sum_{x \in V_j} \mu_i x_i / \sum_{x \in V_j} \mu_i$ . // 2. Update  $\mathbf{y}$ 
  until  $\mathbf{y}$  converges.
  return  $\mathbf{y}, \mathbf{V}(\mathbf{h})$ .
end

```

$$H\delta\mathbf{h} = \nabla E(\mathbf{h}), \quad (7)$$

and update $\mathbf{h} \leftarrow \mathbf{h} + \sigma\delta\mathbf{h}$. We show the complete algorithm for obtaining the OT-Map $\pi : X \rightarrow Y$ in Alg. 1.

5 Variational Wasserstein Clustering

We now introduce in details our method to solve clustering problems through variational optimal transportation. We name it *variational Wasserstein clustering*. We focus on the semi-discrete clustering problem which is to find a set of discrete sparse centroids to best represent a continuous probability measure, or its discrete empirical representation. Suppose X is a metric space and we embody it with an empirical measure $(\mathbf{x}, \boldsymbol{\mu})$. Now, our goal is to find a discrete measure $(\mathbf{y}, \boldsymbol{\nu})$ in Y such that Eq. (3) reaches its minimum.

We begin with an assumption that the distributional data are embedded in the same space, i.e. $X = Y$. We observe that if $\boldsymbol{\nu}$ is fixed then Eq. (2) and Eq. (3) are mathematically equivalent. Thus, the computational approaches to these two problems could also coincide. Because the space is convex, each cluster is a Voronoi cell and the resulting partition from the clustering is actually a *power Voronoi diagram*, or *power diagram* where we have $x \in V_i$, $\|x - y_i\|^2 - r_i^2 \leq \|x - y_j\|^2 - r_j^2$, $\forall i \neq j$ and r is controlled by the total mass of each cell. Such a diagram is also the solution to Monge's OT problem between $(\mathbf{x}, \boldsymbol{\mu})$ and $(\mathbf{y}, \boldsymbol{\nu})$. From the previous section, we know that if \mathbf{x} and \mathbf{y} are fixed the power diagram is entirely determined by the minimizer \mathbf{h} . Thus, when $\boldsymbol{\nu}$ is fixed and \mathbf{y} is allowed to move freely in X , we reformulate Eq. (3) to

$$f(\mathbf{y}, \mathbf{h}) = \sum_{j=1}^K \sum_{x_i \in V_j(\mathbf{h})} \mu_i \|x_i - y_j\|^2. \quad (8)$$

The solution in Eq. (8) can be achieved by iteratively updating \mathbf{h} and \mathbf{y} . While we can use Alg. 1 to compute \mathbf{h} , updating \mathbf{y} can follow the rule:

$$y_j^{(t+1)} \leftarrow \sum \mu_i x_i^{(t)} / \sum \mu_i, \quad x_i^{(t)} \in V_j. \quad (9)$$

Algorithm 3: Variational Wasserstein clustering

Input : Empirical measures $X(\mathbf{x}, \boldsymbol{\mu})$ and $Y(\mathbf{y}, \boldsymbol{\nu})$
Output: Measure-preserving Map $\pi : (\mathbf{x}, \boldsymbol{\mu}) \rightarrow (\mathbf{y}, \boldsymbol{\nu})$, represented as $V(\mathbf{y}, \boldsymbol{\nu}, \mathbf{h})$.

begin
 $\boldsymbol{\nu} \leftarrow$ Sampling-known-distribution.// Initialization.

 Harmonic-mapping: $X, Y \rightarrow \mathbb{R}^n, \mathbb{S}^n$ or \mathbb{D}^n // Unify domains.

 $\mathbf{y}, \mathbf{V} \leftarrow$ Iterative-Measure-Preserving-Mapping($\mathbf{x}, \boldsymbol{\mu}, \mathbf{y}, \boldsymbol{\nu}$).

end
return \mathbf{y}, \mathbf{V} .

Since the first step preserves the measure and the second step update the measure, we call such a mapping an *iterative measure-preserving mapping*. Our algorithm repeatedly updates the Voronoi partition of the space by variational-OT and computes the new centroids until convergence, as shown in Alg. 2. Furthermore, because each step reduces the total transportation cost (8), we have the following propositions.

Proposition 1. *Alg. 2 monotonically minimizes the object function (8).*

Proof. It is sufficient for us to show that for any $t \geq 0$, we have

$$f(\mathbf{h}^{(t+1)}, \mathbf{y}^{(t+1)}) \leq f(\mathbf{h}^{(t)}, \mathbf{y}^{(t)}). \quad (10)$$

The above inequality is indeed true since $f(\mathbf{h}^{(t+1)}, \mathbf{y}^{(t)}) \leq f(\mathbf{h}^{(t)}, \mathbf{y}^{(t)})$ according to the convexity of our OT formulation, and $f(\mathbf{h}^{(t+1)}, \mathbf{y}^{(t+1)}) \leq f(\mathbf{h}^{(t+1)}, \mathbf{y}^{(t)})$ for the updating process itself minimizes the mean squared error. \square

Proposition 2. *Alg. 2 converges in a finite number of iterations.*

Proof. We borrow the proof for k-means. Given N empirical samples and a fixed number k , there are k^N ways of clustering. At each iteration, our method Alg. 2 produces a new clustering rule only based on the previous one. The new clustering rule induces a lower cost if it is different than the previous one, or the same cost if it is the same as the previous one. Since the domain is a finite set, the iteration must eventually enter a cycle whose length cannot be greater than 1 because otherwise it violates the fact of the monological declining cost. Therefore, the cycle has the length of 1 in which case the algorithm converges in a finite number of iterations. \square

Corollary 1. *Alg. 2 produces a unique solution to Eq. (8).*

Now, we introduce the concept of variational Wasserstein clustering. For a subset $M \subset \mathbb{R}^n$, let $P(M)$ be the space of all Borel probability measures. Suppose $X(\mathbf{x}, \boldsymbol{\mu}) \in P(M)$ is an existing probability measure on M and we are to aggregate it into k clusters represented by another probability measure

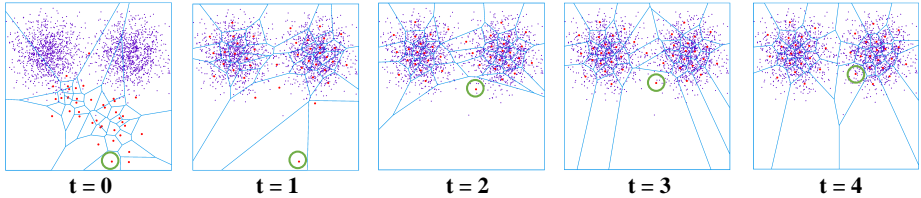


Fig. 2. The distribution with k discrete measures are driven into the target distribution to form a Voronoi diagram that partitions the domain into k clusters. The diagram is being updated to minimize the total mapping cost from the target distribution to the source distribution. The green circle is tracking a centroid.

$Y(\mathbf{y}, \nu) \in P(M)$ and the assignment $y_j = \pi(x_i)$, $j = 1, \dots, k$. Thus, we have $Y \in P(M)$ and $\pi \in P(M \times M)$. Given ν fixed, our goal is to find such a probability $Y_{\mathbf{y}, \nu}$ and assignment $\pi : \mathbf{x} \rightarrow \mathbf{y}$ that minimize the object function:

$$Y_{\mathbf{y}, \nu} = \underset{\substack{Y \in P(M) \\ \pi \in P(M \times M)}}}{\operatorname{argmin}} \sum_{j=1}^k \sum_{y_j = \pi(x_i)} \mu_i \|x_i - y_j\|^2, \text{ s.t. } \nu_j = \sum_{y_j = \pi(x_i)} \mu_i. \quad (11)$$

Eq. (11) is not convex w.r.t. \mathbf{y} as discussed in [5]. We thus solve it by iteratively updating \mathbf{y} and π . When updating π , since \mathbf{y} is fixed, Eq. (11) becomes an optimal transportation problem. Therefore, solving Eq. (11) is equivalent to approaching the infimum of the 2-Wasserstein distance between $X(\mathbf{x}, \mu)$ and $Y(\mathbf{y}, \nu)$.

$$\inf_{\substack{Y \in P(M) \\ \pi \in P(M \times M)}} \sum_{j=1}^k \sum_{y_j = \pi(x_i)} \mu_i \|x_i - y_j\|^2 = \inf_{Y \in P(M)} W_2^2(X, Y). \quad (12)$$

Because the domain is convex, we can apply iterative measure-preserving mapping (Alg. 2) to obtain \mathbf{y} and \mathbf{h} which induces π . We wrap up our complete algorithm in Alg. 3. In case that X and Y are not in the same domain i.e. $Y(\mathbf{y}, \nu) \in P(N)$, $N \subset \mathbb{R}^n$, $N \neq M$, or the domain is not necessarily convex, we leverage *harmonic mapping* to map them to a convex canonical space. The computational algorithms can be found in [26,27]. Fig. 2 illustrates the deformation of the centroids and the clusters during the first four iterations. The green circle in the figure is tracking a centroid starting from the bottom. After the first iteration (2nd picture from the left), there is not any observation in its cluster, so we do not change its position. We implement our algorithm in C/C++ and adopt voro++ [28] to compute Voronoi diagrams.

6 Applications

While the k-means clustering problem is ubiquitous in numerous tasks in computer vision and machine learning, in this section we present the use of our

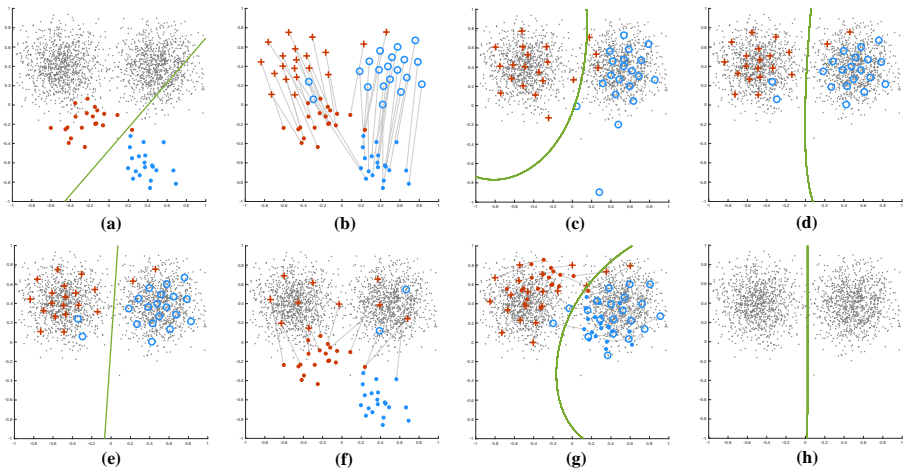


Fig. 3. Classification decision boundaries from domain adaptation with different methods. (a) Original target domain in gray dots while source domain with two classes in red and blue dots; (b) Mapping of centroids by using our clustering method; (d,e) SVM decision boundaries produced by the final centroids of our method with linear and RBF kernels, respectively; (c) result from our method without iterative centroid update. (f) k-means++ [30] fails to produce classification model; (g) After recentering source domain and target domain, k-means yields acceptable boundary; (h) RBF decision boundary from [10], final centroids not available.

method in approaching domain adaptation, remeshing, and representation learning.

6.1 Domain Adaptation on Synthetic Data

Domain adaptation plays a fundamental role in knowledge transfer and has numerous applications in different fields such image processing and computer vision. Several works have coped with domain adaptation problem by transforming data distributions in order to make them closer with respect to a measure. In recent years, Courty *et al.* [29] took the first steps in applying optimal transportation to domain adaptation. Here we revisit this idea and provide the our own solution to *unsupervised many-to-one domain adaptation* based on variational Wasserstein clustering.

Consider a two-class classification problem in the 2D Euclidean space. The source domain consists of two independent Gaussian distributions sampled by red and blue dots as shown in Fig. 3 (a). Each class has 20 samples. The target domain has two other Gaussian distributions with different means and variances, each having 1000 samples. They are represented by denser gray samples to emulate the source domain after an unknown transformation.

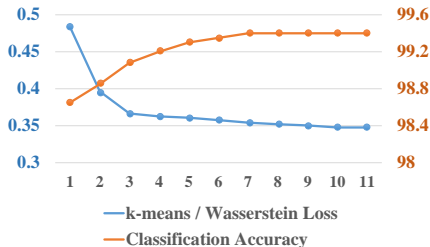


Fig. 4. Clustering loss and accuracy over iterations, for testing applicability to domain adaptation on synthetic data.



Fig. 5. Classification accuracies of VWC and PCA on AD and NC w.r.t. number of components.

We adopt support vector machines (SVMs) with linear and RBF kernels for classification. One can notice that directly applying the linear classifier learned from the source domain to the target domain provides a poor classification result (58.55%). While Fig. 3 (b) shows the final positions of the samples from the source domain, (d) and (e) show the decision boundaries from SVMs with a radial basis function (RBF) kernel and a linear kernel, respectively. We also show in (c) the result from our algorithm without iterative centroid update as a comparison with (d). In (f) and (g) we test the classic k-means++ method [30]. In (f) k-means++ fails to cluster the unlabeled samples into the original source domain and produces a fully biased model that has 50% of accuracy. Only after we recenter the source and target domains yields k-means++ better results. We also show the decision boundary obtained from JDOT [10] in (h). Since JDOT uses Sinkhorn [13] for computing optimal transportation, the final centroids are not available. In this experiment, both our method for Monge’s OT problem and the methods [10,7] for Kantorovich’s OT problem can successfully transfer knowledges between different domains, while the traditional method [30] can only work after a prior knowledge between the two domains, e.g. a linear offset. Detailed performance is reported in Tab. 1. All the results were obtained from 5 fold cross-validation. We also show the clustering loss and RBF classification accuracy over iterations in Fig. 4.

One can notice that the decision boundary from [10] (g) is almost straight even under a RBF kernel, which is more coherent with the shape of the target domain than ours (d). That is probably because its mapping is regularized by the original labels so that the two distributions – red and blue – are bounded during the mapping. This is reflected in (d) that two centroids in each class are misplaced and far away from the rest of their own classes. This could be a further work on top of our method to improve the performance.

6.2 Deforming Triangle Meshes

Triangle meshes is a dominant approximation of surfaces. Refining triangle meshes to best represent surfaces have been studies for decades, including [31,32,33].

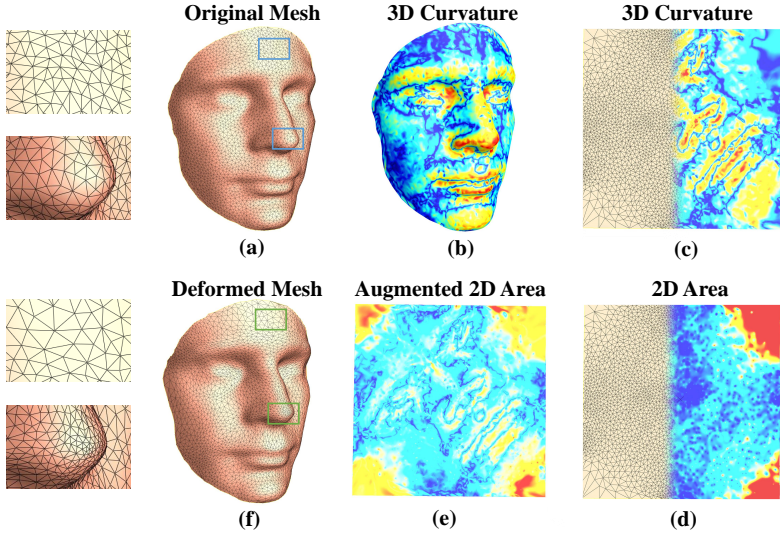


Fig. 6. Redistribute triangulation based on curvature. (b) shows the curvature (\mathbf{x}, \mathbf{c}) on 3D surface. Surface is mapped to 2D planar domain (c), curvature is copied from 3D. Design an empirical measure ($\mathbf{x}', \boldsymbol{\mu}$) on the 2D plane by incorporating curvature \mathbf{c} into the 2D vertex area \mathbf{a} , e.g. $\boldsymbol{\mu} = 0.4\mathbf{a} + 0.6\mathbf{c}$ as in (e). For a vertex y_i with a large curvature on 2D domain, in order to maintain its original measure a_i , it will shrink its own cluster. As a result vertices will aggregate in high curvature locations (f).

Given limited storage, we prefer to use denser and smaller triangles to represent curvy areas and sparser and larger triangles for flat regions. We follow this direction and propose to use our method for solving this problem. The idea is to drive the vertices toward highly curvy regions. We consider a surface \mathbb{S}^2 approximated by a triangle mesh $T^{(1)}(\mathbf{v})$.

To drive the vertices to high curvature positions, our general idea is to reduce the areas of the triangles in there and increase them in those locations of low curvature, producing a new triangulation $T^{(2)}(\mathbf{v})$ on the surface. To avoid

Table 1. Classification Accuracy for Domain Adaptation on Synthetic Data

Kernel	k-means++*		k-means++ [†]		JDOT		VWC ¹		VWC	
	Linear/RBF	Linear RBF	Linear RBF	RBF	Linear RBF	RBF	Linear RBF	RBF	Linear RBF	RBF
Accuracy	50.00	98.55	98.45	99.45	99.30	98.85	98.65	99.35	99.40	
Sensitivity	50.00	98.40	98.30	99.60	99.50	99.10	99.00	99.60	99.60	
Specificity	0.00	98.70	98.60	99.30	99.10	98.60	98.30	99.10	99.20	

*: fully biased model labeling all samples with same class; [†]: recentered; ¹: after 1 iteration.

computing the geodesic on the surface, we first do harmonic mapping from the surface to a unit square $\phi : \mathbb{S} \rightarrow \mathbb{Q}$. For simplicity, we drop the superscripts, 2. To clarify notations, we use $T_{\mathbb{S}}^{(1)}(\mathbf{v})$ to represent the original triangulation on surface \mathbb{S} ; $T_{\mathbb{Q}}^{(1)}(\mathbf{v})'$ to represent its counterpart on \mathbb{Q} after harmonic mapping; $T_{\mathbb{Q}}^{(2)}(\mathbf{v})'$ for the target triangulation on \mathbb{Q} and $T_{\mathbb{S}}^{(2)}(\mathbf{v})$ on S . Fig. 6 (a) and (c) illustrate the triangulation before and after the harmonic mapping. Our goal is to rearrange the triangulation on \mathbb{Q} and then the composition gives the designed triangulation the surface:

$$T_{\mathbb{S}}^{(1)}(\mathbf{v}) \xrightarrow{\phi} T_{\mathbb{Q}}^{(1)}(\mathbf{v}) \xrightarrow{\pi} T_{\mathbb{Q}}^{(2)}(\mathbf{v}) \xrightarrow{\phi^{-1}} T_{\mathbb{S}}^{(2)}(\mathbf{v}).$$

π is where we apply our method. First, we compute the area $A_{\mathbb{Q}} : \mathbf{v} \rightarrow \mathbf{a}$ of each vertex on \mathbb{Q} . This is the source measure. To obtain the target measure which should have more samples on Q , we subdivide $T_{\mathbb{S}}^{(1)}(\mathbf{v})$ into $T_{sub, \mathbb{S}}^{(1)}(\mathbf{v}_{sub})$ and then compute the mean curvature $C_{sub, \mathbb{S}} : \mathbf{v}_{sub} \rightarrow \mathbf{c}_{sub}$ of each vertex on \mathbb{S} and the area $A_{sub, \mathbb{S}} : \mathbf{v}_{sub} \rightarrow \mathbf{a}_{sub}$ on Q . After normalization, a weighted summation gives us the target measure $\mathbf{x}_{sub} = (1 - \lambda) \mathbf{a}_{sub} + \lambda \mathbf{c}_{sub}$.

Now, we start from the source measure (\mathbf{v}, \mathbf{a}) and cluster the target measure $(\mathbf{v}_{sub}, \mathbf{x}_{sub})$. The intuition is the following. If $\lambda = 0$, $x_{i,sub} = a_{i,sub}$ everywhere, then a simple unweighted Voronoi diagram which is the dual of $T_{\mathbb{Q}}^{(1)}(\mathbf{v})$ would satisfy Eq. (11) and (12). As λ is increasing, the clusters $V_j(t_j, a_j)$ in the high curvature locations will require smaller regions to satisfy $a_j = \sum_{v_{i,sub} \in V_j} x_{i,sub}$.

We apply our method on a human face for validation and show the result in Fig. 6. On the left we show the comparison before and after remeshing. The tip of the nose have more triangles due to the high curvatures while the forehead becomes sparser because it is relatively flatter. The right half of Fig. 6 shows different measures that we computed for driving the vertices of the mesh. (b) shows the mean curvature on the 3D surface. We map the triangulation with the curvature onto the planar domain (c). (d) illustrates the vertex area of the planar triangulation and (e) is the weighted combination of 3D curvature and 2D area. Finally, we regard 2D area (d) as the source domain and the ‘‘augmented’’ area (e) as the target domain and apply our method to obtain the new arrangement of the vertices on the planar domain. After that we pull it back to 3D surface. As a result vertices are attracted into high curvature areas.

6.3 Learning Representations of Brain Images

Millions of voxels contained in a 3D brain image bring efficiency issues for computer-aided diagnoses. A good learning technique can extract a better representation of the original data in the sense that it reduces the dimensionality and/or enhances important information for further processes. In this section, we address learning representations of brain images from a perspective of Wasserstein clustering and verify our algorithm on magnetic resonance imaging (MRI).

In the high level, given a brain image $X(\mathbf{x}, \boldsymbol{\mu})$ where \mathbf{x} represents the voxels and $\boldsymbol{\mu}$ their intensities, we aim to cluster the image with a known sparse

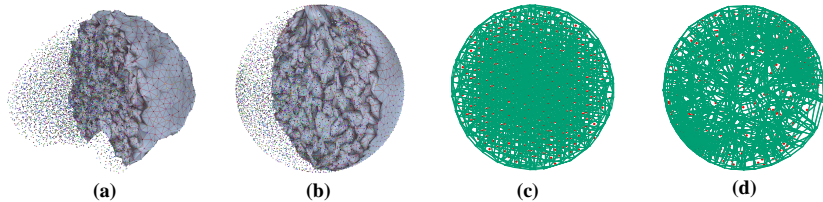


Fig. 7. Brain images are projected to tetrahedral meshes (a) that are generated from brain surfaces. Meshes are deformed into unit balls (b) via harmonic mapping. A sparse uniform distribution inside the ball (c) is initialized and shown with the initial Voronoi diagram. We start from (c) as the initial centroids and cluster (b) as the empirical measure by using our proposed method. (d) shows the resulting centroids and diagram.

distribution $Y(\mathbf{y}, \nu)$. Brain images, particularly MRI, can be treated as distributions. MRI measures the time taken for hydrogen nuclei to return to their original state after excited by external radiofrequency (RF) pulses [34] and thus can be considered as a map of the nuclear energy of the entire brain volume. We consider each brain image representing the brain volume is a submanifold in the 3D Euclidean space, i.e. $X \subset \mathbb{R}^3$. To prepare the data, for each brain image, we first remove the skull and extract the surface of the brain volume by using Freesurfer [35], and use Tetgen [36] to create a tetrahedral mesh from the surface. Then, we project the image onto the tetrahedral mesh by finding the nearest neighbors and perform harmonic mapping to map it to a unit ball as shown in Fig. 7 (a) and (b).

Now, following Alg. 3, we set a discrete uniform distribution sparsely supported in the unit ball, $Y(\mathbf{y}, \nu) \sim U(-1, 1) \cap \mathbb{D}^3$ as shown in Fig. 7 (c). Starting from this, we learn such a new \mathbf{y} that the representation mapping $\pi : \mathbf{x} \rightarrow \mathbf{y}$ has the minimum cost (12). Thus, we can think of this process as a non-parametric mapping from the input to a latent space $P(\mathbf{y})$ of the dimension $k \times n \ll |\mathbf{x}|$ where k is the number of clusters and n specifies the dimension of the original embedding space, e.g. 3 for brain images. Fig. 7 (d) shows the resulting centroids and the corresponding power diagram. We compare our method with PCA to show its capacity in dimensionality reduction in Fig. 5. We apply both method on 100 MRI images with 50 of them labeled Alzheimer’s disease (AD) and 50 labeled normal control (NC). After obtaining the low-dimensional features, we directly apply a linear SVM classifier on them for 5-fold cross-validation. The plots show the significant jump between these two methods. It is well known that people with Alzheimer’s disease suffer whole brain atrophy resulting in a group-wise shift of the corresponding brain images [37]. The result shows the potential of our method in embedding the whole brain image in low-dimensional spaces. Along this direction, we could further incorporate prior knowledge such as regions-of-interest and geometric features such as curvatures into our method by adding regularization and by carefully designing initial centroids.

7 Conclusions and Future Work

Optimal transportation has gained increasingly popularity in recent years thanks to its robustness and scalability in many areas. Built upon variational optimal transportation, we have proposed a clustering technique by solving iterative measure-preserving mapping and demonstrated its applications to different problems in computer vision and machine learning. Future work could include adding regularization to our formulation to improve its robustness. Also, to further improve the performance of our method, it is desirable to incorporate the process of updating the centroids in to our formulation of the optimal transportation, that is simultaneously updating the power diagram and the positions of the centroids.

References

1. Lloyd, S.: Least squares quantization in pcm. *IEEE transactions on information theory* **28**(2) (1982) 129–137
2. Forgy, E.W.: Cluster analysis of multivariate data: efficiency versus interpretability of classifications. *biometrics* **21** (1965) 768–769
3. Graf, S., Luschgy, H.: *Foundations of quantization for probability distributions*. Springer (2007)
4. Agueh, M., Carlier, G.: Barycenters in the Wasserstein space. *SIAM Journal on Mathematical Analysis* **43**(2) (2011) 904–924
5. Cuturi, M., Doucet, A.: Fast computation of wasserstein barycenters. In: *International Conference on Machine Learning*. (2014) 685–693
6. Solomon, J., De Goes, F., Peyré, G., Cuturi, M., Butscher, A., Nguyen, A., Du, T., Guibas, L.: Convolutional wasserstein distances: Efficient optimal transportation on geometric domains. *ACM Transactions on Graphics (TOG)* **34**(4) (2015) 66
7. Ye, J., Wu, P., Wang, J.Z., Li, J.: Fast discrete distribution clustering using Wasserstein barycenter with sparse support. *IEEE Transactions on Signal Processing* **65**(9) (2017) 2317–2332
8. Ho, N., Nguyen, X., Yurochkin, M., Bui, H.H., Huynh, V., Phung, D.: Multilevel clustering via wasserstein means. *arXiv preprint arXiv:1706.03883* (2017)
9. Gu, X., Luo, F., Sun, J., Yau, S.T.: Variational principles for minkowski type problems, discrete optimal transport, and discrete monge-ampere equations. *arXiv preprint arXiv:1302.5472* (2013)
10. Courty, N., Flamary, R., Habrard, A., Rakotomamonjy, A.: Joint distribution optimal transportation for domain adaptation. In: *Advances in Neural Information Processing Systems*. (2017) 3733–3742
11. Monge, G.: *Mémoire sur la théorie des déblais et des remblais*. *Histoire de l’Académie Royale des Sciences de Paris* (1781)
12. Kantorovich, L.V.: On the translocation of masses. In: *Dokl. Akad. Nauk SSSR*. Volume 37. (1942) 199–201
13. Cuturi, M.: Sinkhorn distances: Lightspeed computation of optimal transport. In: *Advances in neural information processing systems*. (2013) 2292–2300
14. Brenier, Y.: Polar factorization and monotone rearrangement of vector-valued functions. *Communications on pure and applied mathematics* **44**(4) (1991) 375–417
15. Su, Z., Wang, Y., Shi, R., Zeng, W., Sun, J., Luo, F., Gu, X.: Optimal mass transport for shape matching and comparison. *IEEE transactions on pattern analysis and machine intelligence* **37**(11) (2015) 2246–2259
16. Givens, C.R., Shortt, R.M., et al.: A class of wasserstein metrics for probability distributions. *The Michigan Mathematical Journal* **31**(2) (1984) 231–240
17. Rubner, Y., Tomasi, C., Guibas, L.J.: The earth mover’s distance as a metric for image retrieval. *International journal of computer vision* **40**(2) (2000) 99–121
18. Ling, H., Okada, K.: An efficient earth mover’s distance algorithm for robust histogram comparison. *IEEE transactions on pattern analysis and machine intelligence* **29**(5) (2007) 840–853
19. Arjovsky, M., Chintala, S., Bottou, L.: Wasserstein generative adversarial networks. In: *International Conference on Machine Learning*. (2017) 214–223
20. Frogner, C., Zhang, C., Mobahi, H., Araya, M., Poggio, T.A.: Learning with a wasserstein loss. In: *Advances in Neural Information Processing Systems*. (2015) 2053–2061

21. Gibbs, A.L., Su, F.E.: On choosing and bounding probability metrics. *International statistical review* **70**(3) (2002) 419–435
22. Applegate, D., Dasu, T., Krishnan, S., Urbanek, S.: Unsupervised clustering of multidimensional distributions using earth mover distance. In: *Proceedings of the 17th ACM SIGKDD international conference on Knowledge discovery and data mining*, ACM (2011) 636–644
23. Villani: *Topics in optimal transportation*. American Mathematical Society **58** (2003)
24. Aurenhammer, F.: Power diagrams: properties, algorithms and applications. *SIAM Journal on Computing* **16**(1) (1987) 78–96
25. Alexandrov, A.D.: *Convex polyhedra*. Springer Science & Business Media (2005)
26. Gu, X.D., Yau, S.T.: *Computational conformal geometry*. International Press Somerville, Mass, USA (2008)
27. Wang, Y., Gu, X., Chan, T.F., Thompson, P.M., Yau, S.T.: Volumetric harmonic brain mapping. In: *Biomedical Imaging: From Nano to Macro, 2004. ISBI 2004. IEEE International Symposium on*. (Apr. 2004) 1275–1278
28. Rycroft, C.: *A three-dimensional Voronoi cell library in C++*. Lawrence Berkeley National Laboratory (2009)
29. Courty, N., Flamary, R., Tuia, D.: Domain adaptation with regularized optimal transport. In: *Joint European Conference on Machine Learning and Knowledge Discovery in Databases*, Springer (2014) 274–289
30. Arthur, D., Vassilvitskii, S.: k-means++: The advantages of careful seeding. In: *Proceedings of the eighteenth annual ACM-SIAM symposium on Discrete algorithms*, Society for Industrial and Applied Mathematics (2007) 1027–1035
31. Shewchuk, J.R.: Delaunay refinement algorithms for triangular mesh generation. *Computational geometry* **22**(1-3) (2002) 21–74
32. Fabri, A., Pion, S.: Cgal: The computational geometry algorithms library. In: *Proceedings of the 17th ACM SIGSPATIAL international conference on advances in geographic information systems*, ACM (2009) 538–539
33. Goes, F.d., Memari, P., Mullen, P., Desbrun, M.: Weighted triangulations for geometry processing. *ACM Transactions on Graphics (TOG)* **33**(3) (2014) 28
34. McRobbie, D.W., Moore, E.A., Graves, M.J.: *MRI from Picture to Proton*. Cambridge university press (2017)
35. <http://freesurfer.net/>
36. Si, H.: Tetgen, a delaunay-based quality tetrahedral mesh generator. *ACM Trans. on Mathematical Software (TOMS)* **41**(2) (2015) 11
37. Fox, N.C., Freeborough, P.A.: Brain atrophy progression measured from registered serial mri: validation and application to alzheimer’s disease. *Journal of Magnetic Resonance Imaging* **7**(6) (1997) 1069–1075